EVALUATION OF HEAT TRANSFER BOUNDARY CONDITIONS FOR CFD MODELING OF A 3D PLATE HEAT EXCHANGER GEOMETRY

T.M. Pääkkönen[1], M. Riihimäki[1], R. Ylönen[1], E. Muurinen[1], C.J. Simonson[2] and R.L. Keiski[1]

[1] University of Oulu, Department of Process and Environmental Engineering, Laboratory of Mass and Heat Transfer Processes, P.O. Box 4300, FI-90014 University of Oulu, Finland, E-mail: tiina.m.paakkonen@oulu.fi
[2]University of Saskatchewan, Department of Mechanical Engineering, Saskatoon, SK, Canada

ABSTRACT

In this paper fluid flow and heat transfer are modeled in a corrugated 3D plate heat exchanger geometry with a commercial computational fluid dynamics (CFD) program, Fluent 6.1.22 (Fluent Inc., Lebanon), in order to find out the most realistic heat transfer boundary conditions for a plate heat exchanger. The built-in boundary conditions of Fluent available for this case are Heat flux, Convection and Constant wall temperature. The CFD models are verified with correlations and experimental data obtained by a flat plate test equipment of which parameters can be calculated analytically.

Deficiencies are found in all the built-in heat transfer boundary conditions. Heat transfer modeling with CFD in a corrugated plate heat exchanger is problematic because of the assumptions that have to be made when defining the boundary conditions in the complex geometry. The values of the computational parameters have spatial variations and can not be defined explicitly. However, when compared to the experimental correlations in the literature, the Convection boundary condition gives the most realistic results in the case of corrugated plate heat exchanger.

INTRODUCTION

Background

New heat exchanger geometries are traditionally developed by the trial and error method using a heuristic approach. Theoretical predictions of the thermal efficiency of plate heat exchangers would facilitate the design of new heat exchangers. Accurate prediction of reactions, heat transfer and fluid flow in different heat exchanger geometries would also help to minimize fouling of heat exchangers.

Fouling, deposition of unwanted material on the heat transfer surface, diminishes the heat transfer and increases the pressure drop. The deposited material lowers the energy efficiency of the heat exchanger by increasing heat transfer resistance. The flow resistance, caused by the fouling layer, increases the pressure drop and thus more pumping power is needed. Because of these factors, energy consumption and operation costs of heat exchangers, which are due to over-sizing, additional cleaning costs and process shut downs, are growing. By decreasing the fouling of heat exchangers, energy consumption and hence climate effects, like carbon dioxide emissions, caused by energy production can be reduced. Other environmental effects are also reduced since the need for chemicals used in cleaning of heat exchangers and the amount of unusable plates are decreased.

Accurate heat transfer modeling is an essential part of fouling models, because temperature has a considerable effect on many fouling mechanisms. Without physically correct boundary conditions neither heat transfer nor fouling can be modeled reliably. The selection of boundary conditions is complicated especially in the case of a complex geometry such as a corrugated plate heat exchanger where the distribution of the local heat transfer coefficient fluctuates (Heggs et al., 1997; Zettler and Müller-Steinhagen, 2001).

Objectives

Reliable heat transfer modeling in corrugated plate heat exchangers is complicated because of local temperature variations on the heat transfer surface. In order to find out the correspondence between experimental and simulated values of heat transfer and pressure drop, the built-in boundary conditions of the simulation software were evaluated.

The objective of this work is to use CDF to model fluid flow and heat transfer in an industrial plate heat exchanger geometry. The aim is also to find the most realistic heat transfer boundary conditions for a corrugated plate heat exchanger and to evaluate the limitations of different boundary conditions. For the verification of the model, flows with Reynolds numbers between 1 650 and 3 100 are investigated and the simulated results are compared with experimental correlations from literature. Fluid flow and heat transfer are also modeled in an ideal flat plate geometry in order to compare the simulation results with experimental data measured in a similar flat plate geometry. The suitability of the flat plate geometry for validation of CFD models is evaluated and also possibility to use it for fouling

model validation is discussed. The obtained information will be useful in later studies when fouling models (Bansal, 1995, Brahim et al. 2003a) are implemented into CFD.

MATERIALS AND METHODS

Structure of the heat exchanger

The corrugated plate heat exchanger studied is a chevron type (Alfa Laval M15-M) with a corrugation angle of 60°. The plate heat exchanger consists of several, vertical, thin, corrugated plates, which are compressed together and sealed with gaskets. In every second plate the corrugated herringbone pattern goes upwards and in every second downwards and hence complicated passages are formed between plates. A corrugated flow channel generates vortices even when the Reynolds number is low. Vortices increase the mixing of the fluid and the heat transfer. In the channels warm and cold flows alternate and heat transfers through the plates by conduction. Heat transfer by forced convection also exists due to the fluid flow. Heat transfer by radiation can be neglected because temperature in the studied heat exchanger is quite low (max. 378 K).

Accurate modeling of the whole plate heat exchanger with CFD is not feasible because of limited computational capacity. For the modeling a small part of the heat exchanger structure, which describes the physical phenomena to be modeled, should be selected. In previous studies other authors (Ciofalo et al., 1996; Mehrabian and Poulter, 2000; Zettler and Müller-Steinhagen, 2001; Islamoglu and Parmaksizoglu, 2006) have used one or two waves in their geometries and periodic boundary conditions to achieve fully developed fluid flow. However, in this case the heat transfer is not periodic, because the temperature is different at the inlet than at the outlet of the channel. Therefore periodic boundary conditions cannot be used for the heat transfer simulation. In this case a larger geometry, which also includes the change of wave direction, is used to ensure a fully developed flow. Thus, one flow channel between two plates of dimensions of 0.14 m x 0.07 m and with several waves is chosen for modeling (Fig. 1). The geometry is meshed with 408 000 unstructured elements since it is not possible to generate structured mesh because of the very complex geometry. Parameters needed in modeling of corrugated case are taken from the case of an industrial plate heat exchanger, where the cool process fluid (outer fluid flowing outside the modeled channel) is heated with warm district heating water (modeled fluid inside the geometry). Fluid properties needed in calculations are obtained by thermal analysis of the heat exchanger (Riihimäki et al., 2004) where the outer fluid values of the calculation parameters have been estimated from process data and defined as constants where needed.

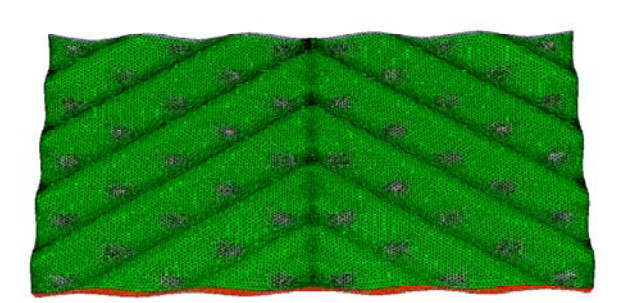

Fig. 1. 3D corrugated plate heat exchanger geometry with a computation mesh.

For validation of the CFD model of the industrial, corrugated plate heat exchanger, also more simple flat plate geometry is generated and modeled. The flat plate geometry with dimensions of 0.1 m x 0.2 m is meshed with 385 000 structured elements (Fig. 2). Also experimental measurements are performed on the same flat plate geometry for model validation. In this case cold water flows through the channel and is heated by ohmic heaters embedded in the walls of the test section. The test section has parallel, heated test sheets which can be changed for analysis and to study different surface materials and structures. The sidewalls of the test section are insulated. The experimental set up has a storage tank, from where the test fluid is circulated through the rectangle test section. The controlled variables in the test system are the fluid flow rate, fluid temperature, and the wall heat flux. The flow rate is measured using a Bürkert 8045 Electromagnetic Flow Transmitter. The temperatures of the inlet and outlet fluids and heated walls are measured with SKS Automaatio Oy K-type thermocouples. The control and data acquisition system is built on the National Instruments Inc. components on compact Field point 2100 platform and uses LabView 8.0 software.

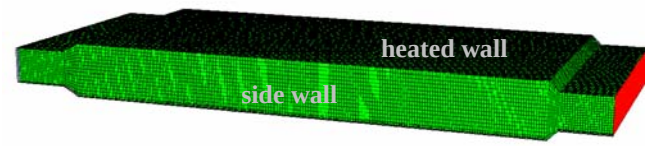

Fig. 2. 3D flat plate heat exchanger geometry with the computation mesh.

Flow model and the boundary conditions for the plate heat exchanger

For the flow conditions in this study, the Reynolds number based on the mean hydraulic diameter of the corrugated flow channel is between 1600 and 3100. According to previous studies in corrugated channels (Mehrabian and Poulter, 2000; Zettler and Müller-

Steinhagen, 2001) the flow field is neither fully laminar nor turbulent and is thus in the transition zone between those Reynolds numbers in this geometry. This may be why different results have been obtained with direct numerical simulation (DNS) and turbulence model. Thus both direct numerical simulation of Navier-Stokes equation and a turbulence model are tested in this study. For turbulence modeling, the RNG k-ε turbulence model is used since it is the most suitable turbulence model for quite small Reynolds numbers, when the flow is not necessarily fully turbulent (Fluent 6.1 User's guide, 2003).

The flow field is solved using the general Navier-Stokes equations presented in Eq. (1) and Eq. (2), from which Eq. (1) is the continuity equation and Eq. (2) is the momentum equation. Equation (3) presents the shear stress tensor in the momentum equation. The temperature field is solved using energy equation in Eq. (4). (Fluent 6.1 User's guide, 2003)

$$\frac{\partial \rho}{\partial t} + \nabla \cdot \left(\rho \bar{u}\right) = S_m \tag{1}$$

$$\frac{\partial}{\partial t}\left(\rho \bar{u}\right) + \nabla \cdot \left(\rho \bar{u}\bar{u}\right) = -\nabla p + \nabla \cdot \bar{\bar{\tau}} + \rho \bar{g} + \bar{F} \tag{2}$$

$$\bar{\bar{\tau}} = \mu\left[\left(\nabla \bar{u} + \nabla \bar{u}^T\right) - \frac{2}{3}\nabla \cdot \bar{u} I\right] \tag{3}$$

$$\frac{\partial}{\partial t}\left(\rho E\right) + \nabla \cdot \left(\bar{u}\left(\rho E + p\right)\right) = \nabla \cdot \left(k_{eff}\nabla T - \sum_j h_j \bar{J}_j + \left(\tau_{eff} \cdot \bar{u}\right)\right) + S_h \tag{4}$$

At the inlet boundary, the flow velocity is specified and at the outlet boundary, the pressure is defined. For the plate walls and the sides of the channel, the no-slip boundary conditions are used. For the heated walls, the thermal boundary conditions are also needed to solve the energy equation.

In this study, the different heat transfer boundary conditions of Fluent 6.1.22 are tested and their applicability in modeling of complicated heat transfer geometry is studied and discussed. The built-in boundary conditions of Fluent 6.1.22 available for this case are Convection, Heat flux and Constant wall temperature.

In the Convection boundary condition, the values of the outer fluid heat transfer coefficient and temperature are defined. The program calculates heat flux to the wall according to Eq. (5) (Fluent 6.1 User's guide, 2003):

$$q = h_f\left(T_w - T_f\right) + q_{rad} = h_{ext}\left(T_{ext} - T_w\right) \tag{5}$$

When using the Heat flux boundary condition an appropriate value for the heat flux at the wall surface is defined and Fluent uses Eq. (6) to calculate the surface temperature of the wall, where the fluid-side heat transfer coefficient (h_f) is computed based on the local flow-field conditions (Fluent 6.1 User's guide, 2003):

$$T_w = \frac{q - q_{rad}}{h_f} + T_f \tag{6}$$

In the Constant wall temperature boundary condition the temperature of the wall is defined and the program calculates the temperature field with Eq. (7) (Fluent 6.1 User's guide, 2003):

$$q = h_f\left(T_w - T_f\right) + q_{rad} \tag{7}$$

RESULTS AND DISCUSSION

Numerical simulations of corrugated geometry compared with experimental correlations

In order to validate the flow model, the fluid flow in the corrugated heat exchanger geometry is modeled with five different flow velocities corresponding to Reynolds numbers of 1 650, 2 020, 2 370, 2 470 and 3 100. Both DNS and RNG k-ε turbulence models are used with these flow velocities. The Fanning friction factor, which determines the pressure drop along the channel, is calculated from the results and plotted as a function of Reynolds number. The simulated results are compared with the results of experimental correlations of Zettler and Müller-Steinhagen (2001). The experimental correlations have been created from measurements on slightly different Alfa Laval plate heat exchanger geometries than the one used in this study. In spite of this, the experimental correlations are used to evaluate the quality of the simulation results. The geometrical parameters of the heat exchanger plates used in this study (plate type M15) and those used in the study of Zettler and Müller-Steinhagen (2001) are shown in Table 1.

Table 1. Geometrical parameters of the plates.

Plate type	Amplitude (m)	Corrugation angle	Wave length (m)
M15	0.0040	60°	0.0140
P01*	0.0012	60°	0.0103
M3*	0.0012	60°	0.0103
M6*	0.0010	60°	0.0110

*Reference: Zettler and Müller-Steinhagen (2001).

The Fanning friction factor determined from the experimental correlations and numerical simulations are

shown in Fig. 3. It can be seen that both the RNG k-ε and the DNS simulation models under-predict the pressure drop and thus the Fanning friction factors, when compared to the correlations. However, it should be mentioned that in the correlation of Zettler (M3) also distributors and ports were included in the measurements. In the correlation of the Alfa Laval (P01), the distribution sector in addition to the flow channel was considered. In that case, the difference compared to the simulations is smaller. The best agreement between the correlations and simulations is achieved when comparing simulations to the correlation of M6 plate in which only the corrugated section has been considered and the dimension of the wavelength is closest to the simulated geometry. It can be noticed that the wave length of the correlation of M6 plate is larger, compared to the other correlations, which usually reduces the pressure drop (Zettler and Müller-Steinhagen, 2001). It should be remarked that also an increase in amplitude usually reduces the pressure drop. Thus, the differences between the experimental correlations and simulations can be partly explained with the differences in geometrical parameters.

The difference between the DNS and the RNG k-ε models is quite small, but the DNS model gives smaller Fanning friction factors, which differs more from experimental correlations. The difference between the DNS and the turbulence models and experimental correlations may indicate that the flow is quite perturbed in the corrugated flow field and computationally too demanding especially for the DNS. This result is consistent with the results of Ciofalo et al. (1996), where it has been found that both turbulence models (standard and low Re number k-ε) and especially DNS under-predicts the pressure drop in intensely corrugated geometries, because the flow is highly perturbed.

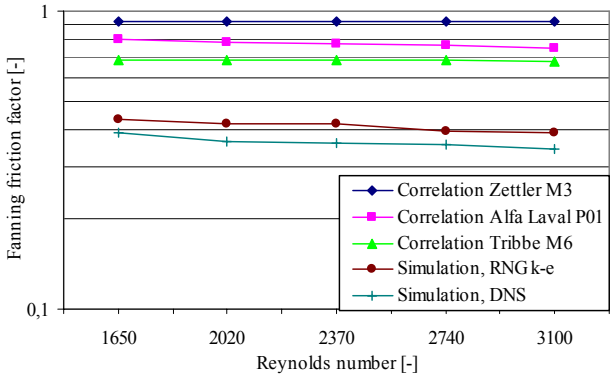

Fig. 3. Comparison of the Fanning friction factors of the experimental correlations of Zettler and Müller-Steinhagen (2001) and the CFD simulations with different Reynolds numbers.

Evaluation and selection of the heat transfer boundary conditions of corrugated geometry

While using the Constant wall temperature boundary condition (Fig. 4) the temperature of the plate is defined to be 353 K, the same as the average temperature of the outer process fluid flowing outside of the geometry. The heat flux through the wall and the temperature field in the geometry are computed. The temperature defined constant at the wall is definitely an inaccurate assumption in this type of heat exchanger because temperature of the fluid on the other side and thus also heat flux changes spatially. The temperature of the plate also has local variations caused by the corrugations.

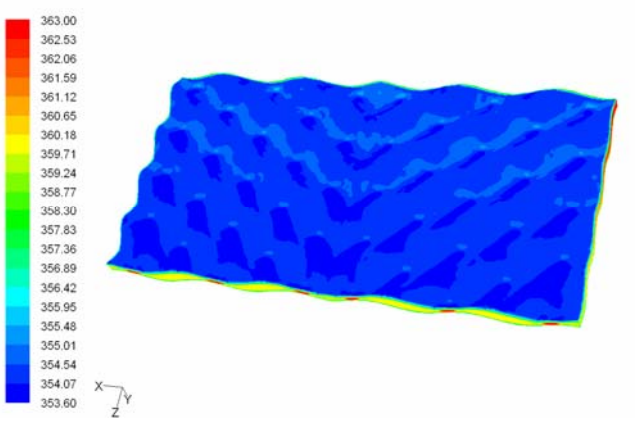

Fig. 4. The temperature field (K) when heat transfer was defined with the Constant wall temperature boundary condition and flow field was calculated with the RNG k-ε - turbulence model (Re = 2740, flow in z-direction).

With the Heat flux boundary condition (Fig. 5), the heat flux has to be defined as a constant at the wall. In this study an empirical Nusselt number correlation with the overall mass and heat balances are used to estimate the heat flux (Riihimäki et al., 2004). The local heat transfer coefficient and furthermore the flux vary spatially at the wall. Thus, the constant heat flux at the wall is not an exact approximation in this case. Furthermore to design a new heat exchanger geometry it would be beneficial to compute the heat flux in order to find out the performance of the structure, not to define it.

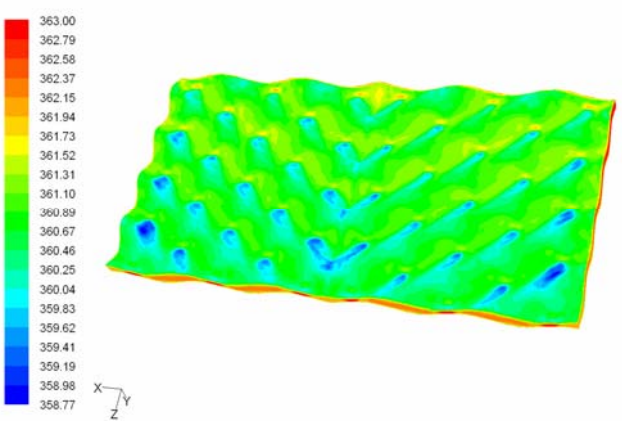

Fig. 5. The temperature field (K) when heat transfer was defined with the Heat flux boundary condition and flow field was calculated with the RNG k-ε -turbulence model (Re = 2740, flow in z-direction).

While using the Convection boundary condition the temperature and the heat transfer coefficient of the outer fluid are defined as constants. The outer fluid, on the other side of the heat exchanger plate has spatial temperature variations similar as flow inside the geometry. However, the heat flux to the wall and the heat transfer coefficient are computed for the fluid inside the modeled channel which means that for the modeled fluid inside the geometry the dependence on temperature and flow rate is being taken into account. Fig. 6 presents the temperature contour of the geometry when heat transfer is calculated with the Convection boundary condition.

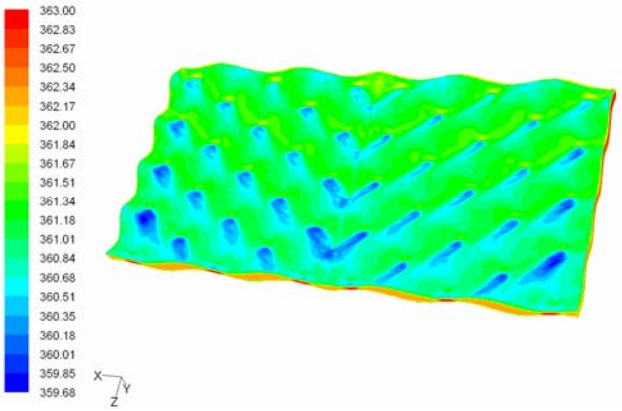

Fig. 6. The temperature field (K) when heat transfer was defined with the Convection boundary condition and flow field was calculated with the RNG k-ε -turbulence model (Re = 2740, flow in z-direction).

The heat transfer calculated with different boundary conditions are presented in Fig. 7. Values of the experimental heat transfer correlation (Marriot, 1971) are also plotted in Fig. 7. Calculation of the experimental correlation is based on an industrial plate heat exchanger (Pääkkönen, 2005). The total heat flux from the correlation is calculated using the overall heat transfer coefficient (Eq. 8) and temperature difference in the studied industrial plate heat exchanger. Nusselt number for the average heat transfer coefficients of water (Eq. 9) and process fluid are calculated from the Marriot's Nusselt number correlation for plate heat exchangers (Eq. 10).

$$q_{tot} = \frac{Q}{A} = U_{tot}\Delta T_{lm} = \left(\frac{1}{\frac{1}{h_{in}} + \frac{1}{h_{ext}} + \frac{\delta}{k}} \right) \Delta T_{lm} \tag{8}$$

$$h = \frac{Nu \cdot k}{D_h} \tag{9}$$

$$Nu = 0.28 \cdot \mathrm{Re}^{0.56} \cdot \mathrm{Pr}^{0.4} \tag{10}$$

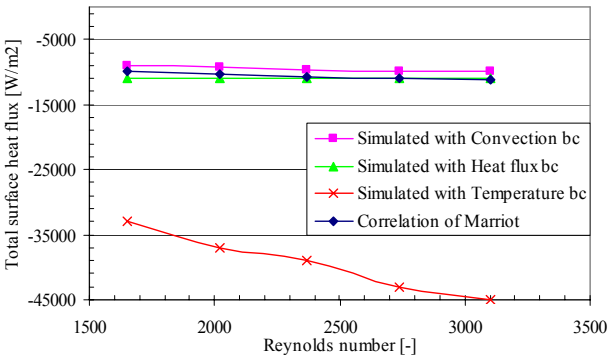

Fig. 7. Comparison of the total heat flux from Marriot's correlation and the CFD simulations with the Convection, Heat flux and Constant wall temperature boundary conditions (bc) as a function of Reynolds numbers.

It can be seen from Fig. 7 that the heat transfer calculated by the Convection boundary condition only slightly underestimates the heat flux. The error is not very large, only about 10 %. With the Heat flux boundary condition the simulated heat flux is constant as expected because it has been defined to the program. In this case, this boundary condition is thus not feasible, because the model should give local variations of the heat flux. Simulations calculated by the Constant wall temperature boundary condition overestimates the heat flux markedly. This is probably due to assumption of constant temperature of the outer fluid. In reality the temperature changes when the heat transfers to the other side of the plate. As a conclusion, the Convection boundary condition gives the most realistic

model for heat transfer in the corrugated plate heat exchanger because it calculates the local variations of heat transfer coefficient and the heat flux.

Evaluation of the heat transfer boundary conditions in the case of the flat plate heat exchanger

The heat transfer CFD model is validated with measurements on a flat plate channel in an experimental setup used in fouling tests. For that purpose the flat plate geometry, describing the experimental setup, is generated and modeled with CFD. In the experimental setup a rectangular channel is heated by ohmic heaters, and no outer fluid exists. That is why the Convection boundary condition is not available for heat transfer modeling of this ideal, flat plate geometry. In this case, only the Heat flux boundary condition is discussed, because it represents the physical situation in the experiments. However in the case of flat plate geometry the constant heat flux could also be quite a good assumption because there are no local variations in heat flux like in the corrugated geometry, but the heat flux changes evenly with the flow field. The RNG k-ε - turbulence model is chosen for modeling of fluid flow in the flat plate geometry, because the flow profile in the channel indicates turbulent flow although there are no vortices in the flow according to CFD simulations. The Reynolds number, which is between 5 200 and 13 800, also indicates that flow is mainly in the transition zone. Generally the flow can be expected to be laminar in this geometry when Reynolds number is below 2 100. Direct numerical simulation is also tested, but the results differed from the experimental results more than results of the turbulence model.

The temperature difference between the inlet and outlet of the test section measured in the experimental setup and calculated in the CFD model of the flat plate geometry are compared to the theoretical temperature difference calculated from a heat balance over the experimental test section in order to evaluate the accuracy of the results. Results are presented in Fig. 8, where the temperature difference between the inflow and outflow is plotted as a function of velocity.

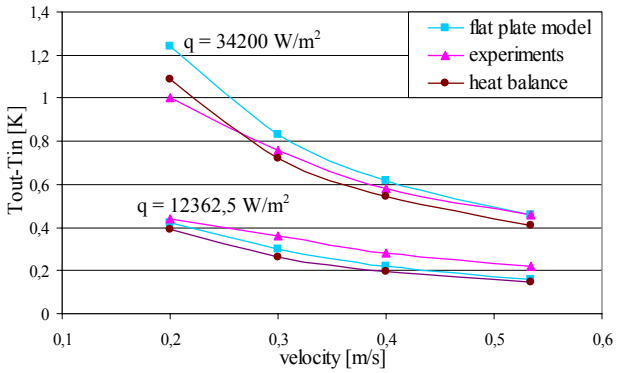

Fig. 8. Temperature difference between the inlet and outlet of the experimental setup and the flat plate geometry model achieved with the Heat flux boundary condition as a function of velocity.

According to the results, the flat plate geometry model with the Heat flux boundary condition predicts quite well the temperature change of the fluid as it flows through the flat plate heat exchanger experimental setup. With a lower heat flux, the model under predicts the temperature difference slightly and with a higher heat flux the model over predicts it especially with smaller velocities. However, small deviations between the experimental and simulated results can be explained with slight inaccuracy in measurements, because results of the CFD model follow theoretical heat balance (brown line in Fig. 8) even better than the experimental results. The inaccuracy in the temperature measurements may derive from incomplete mixing before the thermocouple. As a conclusion the Heat flux boundary condition seems to predict heat transfer quite reliably in the case of flat plate geometry.

The flat plate geometry model is also compared with the result of the corrugated geometry. For this purpose, the inflow velocity and temperature as well as construction material and fluid properties of the corrugated geometry model are defined from physical values of material properties equal to the flat plate geometry model and the experimental setup. The corrugated geometry has different dimensions, which restricts the comparison of the results of different geometries. However, dimensions should not have effect on the heat transfer coefficients and thus it was chosen for comparison.

Heat transfer coefficients on the wall obtained from experimental and numerical data and the values calculated from Nusselt number correlations are plotted in Fig. 9. The results are presented as a function of velocity at two different heat fluxes. The wall heat transfer coefficients are calculated from Eq. 11. The results of the flat plate geometry are also compared to Perry's correlation (1963, p.10–14), which is presented in Eq. 12. Perry's correlation

is for flows in transition zone, where Reynolds number is between 2 100 and 10 000. The results of the corrugated geometry model are compared to Zettler and Müller-Steinhagen's (2001) correlation for corrugated plate heat exchangers, which is presented in Eq. 13.

$$h = \frac{q}{T_w - T_{ref}} \tag{11}$$

$$Nu = 0.116 \cdot \left[\mathrm{Re}^{2/3} - 125 \right] \cdot \mathrm{Pr}^{1/3} \cdot \left[1 + \left(\frac{D_h}{L} \right)^{2/3} \right] \tag{12}$$

$$Nu = 0.38 \cdot \mathrm{Re}^{0.65} \cdot \mathrm{Pr}^{0.33} \tag{13}$$

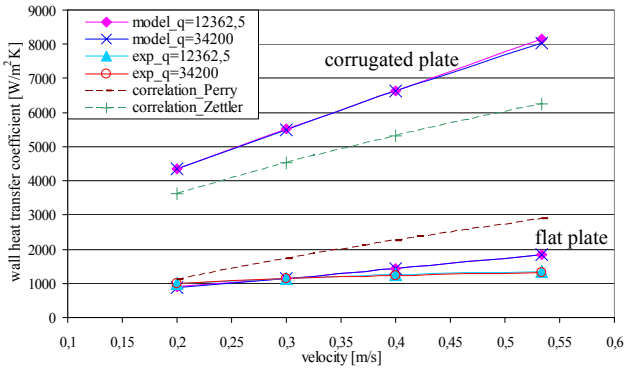

Fig. 9. Heat transfer coefficients as a function of velocity obtained with the experimental tests, and with the flat plate and corrugated geometry models, when Heat flux is used as a boundary condition.

The results show that the flat plate geometry model fits quite well with the experimental result. It seems that the experimental heat transfer coefficients may be too small with higher velocities. The measured wall temperature may differ from the true wall temperature caused by the installation of the thermocouple.

In Fig. 9 Perry's correlation over predicts the wall heat transfer coefficient of the flat plate geometry. The over prediction increases as the velocity increases, and this is probably due to the turbulent nature of the flow, because the Reynolds number is over 13 000 with the highest inflow velocity and thus above the operating range of the correlation. The Zettler and Müller-Steinhagen's correlation gives smaller wall heat transfer coefficients for the corrugated geometry than the CFD model. The deviation is, however, only between 20–28 %. In order to achieve a more suitable correlation for this case, the parameters in the correlation should be fitted case-specifically.

With the same initial conditions, the corrugated geometry gives a higher heat transfer coefficient than the flat plate geometry as expected, since corrugation enhances the heat transfer (Islamoglu and Parmaksizoglu, 2006). In addition, the heat transfer coefficient grows faster as a function of velocity with the corrugated geometry model than with the flat plate geometry model and with the experimental tests.

Based on the results, the corrugated geometry has different flow and heat transfer behavior than the flat geometry. The corrugated plate has an enhanced heat transfer coefficient as well as significant local variations. The structure of the plate also effects to the fouling (Bansal et al., 2000; Brahim et al., 2003b) of plate heat exchangers and thus geometry needs to be taken into account in CFD fouling models.

CONCLUSIONS

With the corrugated geometry, none of the three alternative thermal boundary conditions in Fluent 6.1.22 describe exactly the physical situation in the plate heat exchanger. However, the Convection boundary condition seems to describe most reliably the heat transfer in the corrugated geometry but for the flat plate geometry the Heat flux boundary condition is considered to be the most suitable boundary condition.

In both geometries the results obtained from the CFD model with the appropriate boundary conditions are found to correspond with the results from the experiments and correlations in the literature, especially at lower velocities.

According to this study, it seems that in the future the flat plate geometry could be used in the development and validation of fouling models for flat plate heat exchangers. The fouling model based on the flat plate geometry may then be utilized in modeling of different corrugated geometries. However, because of differences in the flow and heat transfer behavior of a corrugated geometry, the numerical results of fouling in a corrugated geometry will need experimental verification in order to ensure accuracy of the results and further development of the fouling model if necessary.

NOMENCLATURE

D_h hydraulic diameter [m]
F force effecting on the system, for example gravity
h heat transfer coefficient [W/m^2 K]
J diffusion flux of component j [kg/m^2 s]
k conductivity [W/m K]
L length of path of fluid flow [m]
Nu Nusselt number [-]
p pressure [Pa]
Pr Prandtl number [-]
q heat flux [W/m]
Re Reynolds number [-]
S source
t time [s]

T temperature [K]
u flow velocity [m/s]
U_{tot} total heat transfer coefficient [W/m^2 K]

Greek letters

δ thickness of the plate [m]
ρ density [kg/m^3]
$\overline{\overline{\tau}}$ shear stress tensor
μ viscosity [kg/m s]

Subscript

eff effective
ext external
f fluid
in inside
j component
h energy
lm logarithmic mean
m mass
tot total
rad radiation
ref reference
w wall

REFERENCES

Bansal, B., Müller-Steinhagen, H. and Chen, X. D., 2000, Performance of plate heat exchangers during calcium sulphate fouling – investigation with an in-line filter, *Chemical Engineering and Processing*, Vol. 39, p. 507–519.

Bansal, B., 1995, *Crystallization fouling in plate heat exchangers*, PhD Thesis, The University of Auckland, Department of Chemical and Material Sciences, 407 p.

Brahim, F., Augustin, W. and Bohnet, M., 2003a, Numerical simulation of the fouling process, *International Journal of Thermal Sciences*, Vol. 42, p. 323–334.

Brahim, F., Augustin, W. and Bohnet, M., 2003b, Numerical simulation of the fouling on structured heat transfer surfaces (fouling), *The 5th International Conference on Heat Exchanger Fouling and cleaning: Fundamentals and applications*, 18.–22.5.2003, Santa Fe, New Mexico, USA.

Ciofalo, M., Stasiek, J., and Collins, M. W., 1996, Investigation of flow and heat transfer in corrugated passages – II, Numerical simulations, *International Journal of Heat and Mass Transfer*, Vol. 39, (1), p. 165–192.

Fluent, 2003, *Fluent 6.1 User's guide*, Lebanon, Fluent Inc.

Heggs, P. J., Hallam, R. A., and Walton, C., 1997, Local transfer coefficient in corrugated plate heat exchanger channels, *IChemE*, Vol. 75, Part A, p. 641–645.

Islamoglu, Y. and Parmaksizoglu, C., 2006, Comparison of CFD simulation to experiment for convection heat transfer in enhanced channel, *Heat Transfer Engineering*, Vol. 27, (9), p. 53–59.

Marriott, 1971, Where and how to use the plate heat exchanger, *Chemical Engineering*, Vol. 78, April 5, p. 127–134.

Martin, H., 1996, A theoretical approach to predict the performance of chevron-type plate heat exchangers, *Chemical Engineering and Processing*, Vol. 35, (4), p. 301–310.

Mehrabian, M. A., and Poulter, R., 2000, Hydrodynamics and thermal characteristics of corrugated channels: computational approach, *Applied Mathematical Modelling*, Vol. 24, p. 343–364.

Perry, J. H., 1963, *Chemical Engineer's Handbook*, International student edition, USA, McGraw-Hill Inc.

Pääkkönen, T. M., 2005, *Modelling of heat transfer and fluid flow in plate heat exchanger*, Master's thesis, University of Oulu, Department of Process and Environmental Engineering, 117 p.

Riihimäki, M., Muurinen, E., and Keiski, R. L., 2004, Thermal analysis of a plate heat exchanger in fouling conditions – Analysis of process information and calculations based on design equations, *16th International Congress of Chemical and Process Engineering*, 22.–26.8.2004, Prague, Czech Republic.

Zettler, H. U., and Müller-Steinhagen, H., 2001, The use of CFD for the interpretation of fouling data PHEs, *The 4th International Conference on Heat Exchanger Fouling, Fundamental approaches & technical solutions*, 8.–13.7.2001, Davos, Switzerland.